

Ultrahigh detection sensitivity exceeding 10^5 V/W in spin-torque diode

Like Zhang, Bin Fang, Jialin Cai, Mario Carpentieri, Vito Puliafito, Francesca Garesci, Pedram Khalili Amiri, Giovanni Finocchio, and Zhongming Zeng

Citation: *Appl. Phys. Lett.* **113**, 102401 (2018); doi: 10.1063/1.5047547

View online: <https://doi.org/10.1063/1.5047547>

View Table of Contents: <http://aip.scitation.org/toc/apl/113/10>

Published by the [American Institute of Physics](#)

AIP | Conference Proceedings

Get **30% off** all
print proceedings!

Enter Promotion Code **PDF30** at checkout



Ultrahigh detection sensitivity exceeding 10^5 V/W in spin-torque diode

Like Zhang,^{1,2} Bin Fang,¹ Jialin Cai,^{1,2} Mario Carpentieri,³ Vito Puliafito,⁴ Francesca Garescì,⁵ Pedram Khalili Amiri,⁶ Giovanni Finocchio,^{4,a)} and Zhongming Zeng^{1,2,a)}

¹Key Laboratory of Nanodevices and Applications, Suzhou Institute of Nano-Tech and Nano-Bionics, CAS, Suzhou, Jiangsu 215123, People's Republic of China

²School of Nano Technology and Nano Bionics, University of Science and Technology of China, Hefei, Anhui 230026, People's Republic of China

³Department of Electrical and Information Engineering, Polytechnic of Bari, Bari 70125, Italy

⁴Department of Mathematical and Computer Sciences, Physical Sciences and Earth Sciences, University of Messina, Messina 98166, Italy

⁵Department of Engineering, University of Messina, Messina 98166, Italy

⁶Department of Electrical Engineering and Computer Science, Northwestern University, Evanston, Illinois 60208, USA

(Received 9 July 2018; accepted 19 August 2018; published online 4 September 2018)

Microwave detection has a huge number of applications in physics and engineering. It has already been shown that biased spin torque diodes have performance overcoming the CMOS counterpart in terms of sensitivity. In this regard, the spin torque diodes are promising candidates for the next generation of microwave detectors. Here, we show that the optimization of the rectification process based on the injection locking mechanism gives an ultrahigh sensitivity exceeding 200 kV/W with an output resistance below 1 k Ω while maintaining the advantages over other mechanisms such as vortex expulsion or non-linear resonance, to work without a bias magnetic field. *Published by AIP Publishing.* <https://doi.org/10.1063/1.5047547>

In recent years, spin-transfer torque (STT)^{1,2} based devices, such as oscillators^{3,4} and detectors,⁵ have attracted intensive interest in microwave related applications especially for telecommunications, radar technology, high-speed sensors, etc. The physical principle at the basis of an STT-microwave detector is the spin-torque diode effect discovered in 2005 by Tulapurkar *et al.*⁵ Initially, the spin-torque diode effect was used for the electrical characterization of the ferromagnetic resonance response and for the quantitative measurements of magnetic torques in magnetic tunnel junctions (MTJs) (e.g., damping-like, field-like, and voltage-controlled torques).^{6–9} However, many effort measures, such as development of a material structure with a high magnetoresistance (MR) ratio,¹⁰ optimization of the magnetic field direction,^{11–18} application of d.c. bias,¹⁹ and voltage-torque,⁸ have driven a significant improvement in the detection sensitivity. For example, a sensitivity of 12 kV/W was demonstrated by using nonlinear resonance,¹⁹ while 80 kV/W was recently achieved by utilizing the spin-torque induced vortex-core expulsion.²⁰ However, both approaches need a very large external magnetic field applied in a particular direction in order to achieve this large detection sensitivity. Although the external field may in principle be integrated into the device, it is undesirable from a practical point of view due to the increased size and cost. In our previous work,²¹ we demonstrated that a giant detection sensitivity of over 70 kV/W can be achieved by taking advantage of the injection locking between the d.c. driven self-oscillation and the microwave signal in hybrid magnetic tunnel junctions with a perpendicularly magnetized free layer and an in-plane polarizer.

In this study, we show an ultrahigh detection sensitivity of 210 kV/W in the absence of the external magnetic fields. This is arisen from a systematic study of the detection properties by adjusting the CoFeB free layer thickness (additional data from the devices with different CoFeB free layer thicknesses are shown in the [supplementary material](#)), thus optimizing the interfacial perpendicular magnetic anisotropy (IPMA) and the shape anisotropy (cross section geometry) of the spin torque diodes. The origin of this result is the excitation of a large-amplitude out-of-plane magnetization precession in the injection locking region.

The MTJ multilayer stack with a layer structure of bottom contact/seed layer/PtMn (15)/Co₇₀Fe₃₀ (2.3)/Ru (0.85)/Co₄₀Fe₄₀B₂₀ (2.4)/MgO (0.8)/Co₂₀Fe₆₀B₂₀ (1.62)/top contact (numbers are nominal thickness in nanometers) was deposited on a thermally oxidized silicon substrate using a magnetron sputtering system and annealed at 300 °C for 2.0 h in a magnetic field of 1 T. The Co₂₀Fe₆₀B₂₀ free layer was designed by controlling the IPMA field, which almost compensated for the out-of-plane demagnetization field and made the total anisotropy of the film small. The films were subsequently patterned into ellipse-shaped pillars with dimensions of 150 nm \times 50 nm using electron-beam lithography and ion milling techniques. The RF current and d.c. current were applied to the device through a bias Tee using a signal generator (N5183B, Keysight) and a source meter (2400, Keithley), and the spin-torque diode voltage is simultaneously recorded using a lock-in amplifier.

Figures 1(a) and 1(b) show the resistances of one representative device as a function of the magnetic field applied along the plane of the film ($H_{||}$) and normal to the film (H_{\perp}), respectively. $H_{||}$ was applied parallel to the magnetic easy axis of the nanopillar. When $H_{||}$ increases from negative

^{a)}Authors to whom correspondence should be addressed: gfinocchio@unime.it and zmzeng2012@sinano.ac.cn

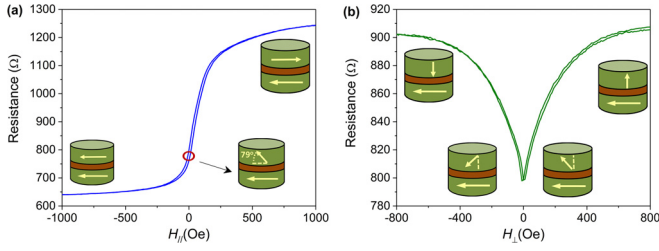


FIG. 1. (a) and (b) The magnetoresistance curve of the MTJ device under the in-plane magnetic field (H_{\parallel}) and the perpendicular magnetic field (H_{\perp}), respectively.

(−1000 Oe) to positive (+1000 Oe), the resistance changes gradually from a low resistance (LR) state to a high resistance (HR) state, indicating that the free-layer magnetization gradually aligns from parallel towards antiparallel to the reference layer magnetization. This is different from the switching behavior that the resistance suddenly changes from a low resistance state to a high resistance state for the in-plane structure.⁵ The feature exhibiting gradually a change in the resistance confirms that the free layer has canted the easy axis at zero magnetic field, which is consistent with the previous report in the presence of easy-cone anisotropy.²² This is also in agreement with the fact that only a small change in the resistance is observed when the magnetic field is applied normal to the film, which corresponds to the slight change in the free-layer magnetization as shown in Fig. 1(b). The exact angle θ between the magnetization vectors of the free and reference layers is estimated to be 79° at zero magnetic field from the magnetoresistance curve²¹ as shown in Fig. 1(a). The resistance-area product in the parallel magnetization configuration was $3.4 \Omega \cdot \mu\text{m}^2$, and the in-plane magnetoresistance (MR) ratio, defined as $(R_{\text{AP}} - R_{\text{P}})/R_{\text{P}}$, was 93%, where the resistances in the anti-parallel (R_{AP}) and parallel (R_{P}) configurations are 1,244 and 640 Ω , respectively. This device design enables the microwave operation in the absence of an applied external magnetic field.

We first studied the detection response of the corresponding device shown in Fig. 1 without applying d.c. bias current. Figure 2(a) shows the detection voltages (V_{dc}) as a function of input RF frequency for various incident RF input powers (P_{RF}). Each spectrum in Fig. 2(a) exhibits a resonant peak, corresponding to the ferromagnetic resonant (FMR) peak of the free layer. The FMR spectra are well fitted by a sum of symmetric and antisymmetric Lorentzian functions. The origin of the asymmetric lineshape is related to the voltage-controlled magnetic anisotropy (VCMA) effect.⁸ At $P_{\text{RF}} = 0.1 \mu\text{W}$, the measured detection sensitivity (defined as $\varepsilon = V_{\text{dc}}/P_{\text{RF}}$) corresponding to the maximum ($f_0 = 1.0$ GHz) of the resonant curve was obtained to be 340 V W^{-1} , which is of the same order as those in previous works.^{8,19,21}

Figure 2(b) shows the detection voltages as a function of the input microwave frequency for various d.c. bias currents under $P_{\text{RF}} = 0.1 \mu\text{W}$. It can be seen that the application of a d.c. bias current to the device can drastically change the detection behavior, as demonstrated in our previous work.²¹ When comparing the data with the FMR mode shown in Fig. 2(a), the first qualitative difference is that the rectification curve is positive for the whole range of frequencies with a

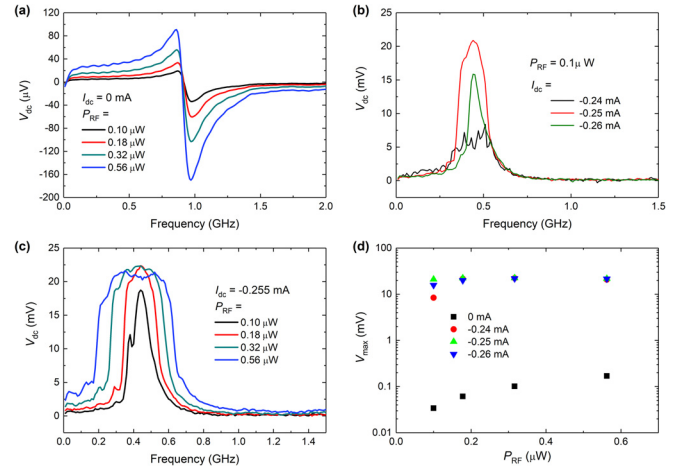


FIG. 2. (a) The detection voltages (V_{dc}) as a function of input RF for various incident RF powers (P_{RF}) under $I_{\text{dc}} = 0 \text{ mA}$. (b) The detection voltages (V_{dc}) as a function of input RF for various d.c. bias currents under $P_{\text{RF}} = 0.1 \mu\text{W}$. (c) Detection voltage (V_{dc}) as a function of RF frequency, for different input microwave powers (P_{RF}) at d.c. bias currents $I_{\text{dc}} = -0.255 \text{ mA}$. (d) RF power (P_{RF}) dependence of maximum detection voltage (V_{max}) at different d.c. bias currents.

shape that is well described only by a symmetric Lorentzian function. The frequency corresponding to the maximum of spectra shifts from 1.0 GHz (FMR mode) to smaller values (non-FMR mode). A systematic scanning of the maximum detected voltage as a function of the bias current clearly shows a significant enhancement as compared with the unbiased results. For example, at $I_{\text{dc}} = -0.255 \text{ mA}$, the rectified voltage reaches 21 mV, corresponding to a detection sensitivity of 210 kV/W , which is the highest value reported to date. Then, we fixed this value of the d.c. bias current and measured the detection voltages at different RF input powers as shown in Fig. 2(c). The measured d.c. voltages first increase with the RF powers and then almost saturate when the RF powers continuously increased [see Fig. 2(d)]. Those measurements are the clear evidence that the detection mechanism underlining this huge detection property is the injection locking.^{21,23} Additional measurements of the microwave emission spectra (not shown here) as a function of the bias current ($I_{\text{RF}} = 0 \text{ mA}$) confirm the excitation of auto-oscillations of the magnetization.²¹

The large enhancement of detection voltage and its dependence on the RF input power can be understood by considering two contributions at the total detection voltage. In the absence of d.c. bias current, the RF input results in a regular FMR oscillation where the precession trajectory behaves at a small angle as shown in Fig. 3(a), thus leading to small detection voltages. In contrast, when a d.c. bias is injected into the MTJ device, at an appropriate condition, spin-torque induced by d.c. current compensates the Gilbert losses, driving the free layer into the large-amplitude out-of-plane precession where the precession trajectory encircles both high resistance and low resistance states as shown in Fig. 3(b). Simultaneously, when the RF inputs with frequencies are similar to the frequencies of these large-amplitude dynamic states, injection locking occurs. The frequency of the locking trajectories can be significantly lower than the FMR frequency of small-amplitude oscillations in the

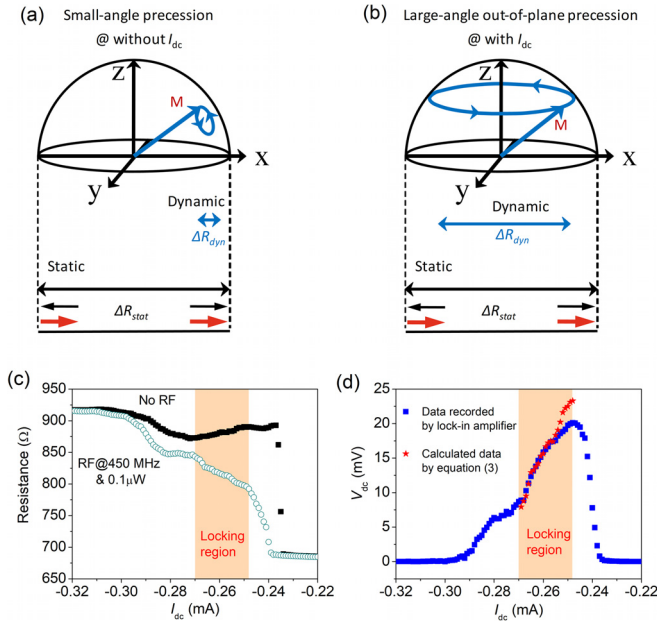


FIG. 3. The schematic of small-angle precession trajectory without I_{dc} (a) and large-angle precession trajectory with I_{dc} (b). (c) Device resistance as a function of I_{dc} with and without the RF drive. (d) The rectified voltage V_{dc} as a function of I_{dc} with the RF drive. The data with stars are calculated data based on Eq. (3).

absence of d.c. current (red-shift tunability), which is in good agreement with our data in Figs. 2(b) and 2(c). Hence, the injection locking leads to an enhanced detection voltage under the simultaneous application of d.c. and RF currents.

Finally, we quantitatively estimate the detection sensitivity of spin-torque diodes in the injection locking condition. Under an RF input, the time-dependent resistance $R(t)$ of spin-torque diodes is given by²⁴

$$R(t) = \Delta R_{dc}(I_{RF}) + \Delta R_s \sin(2\pi f_{RF}t + \Phi_s), \quad (1)$$

where f_{RF} is the RF input frequency, Φ_s is the phase shift between the RF current and the resistance oscillations, $\Delta R_{dc}(I_{RF}) = R_{dc}(I_{RF}) - R_{dc}(0)$ is the difference between the average resistance in the presence and in the absence of I_{RF} , and ΔR_s is the amplitude of the oscillating resistance in the presence of both I_{dc} and I_{RF} . The corresponding detection voltage is given as

$$V_{dc} = 1/\sqrt{2} I_{RF} \Delta R_s \cos(\Phi_s) + I_{dc} \Delta R_{dc}(I_{RF}). \quad (2)$$

Under a weak RF input ($I_{RF} \ll I_{dc}$), the main contribution of Eq. (2) is given by the d.c. contribution

$$V_{dc} \approx I_{dc} \Delta R_{dc}(I_{RF}). \quad (3)$$

To test the validity of Eqs. (2) and (3), we recorded the d.c. resistance and detection voltage as a function of I_{dc} with and without RF input. Figure 3(c) presents an example of device resistance as a function of d.c. bias in the presence and the absence of RF input ($f_{RF} = 450$ MHz and $P_{RF} = 0.1$ μ W). According to Eq. (3) and Fig. 3(c), the d.c. voltage can be computed, which is plotted in Fig. 3(d) (red stars). It can be seen that, in the locking region, the computing values are consistent with the experimental measurements. It is noted that the maximum ΔR_{dc} is approximately equal to the average of

the low resistance (R_P) and high resistance (R_{AP}) states in the large-amplitude out-of-plane oscillation [shown in Fig. 3(b)], and thus, the maximum V_{dc} in the MTJ can be given as $I_{dc}(R_{AP} - R_P)/2$. For the device in this study, the expected maximum V_{dc} can be as high as 75 mV at $I_{dc} = 0.25$ mA. This suggests that there is still room for enhancing the sensitivity by exciting the larger precession cone angle. Furthermore, the sensitivity can be improved by developing MTJs with a higher tunnel magnetoresistance ratio. In addition, it is important to note that there exists an impedance mismatching of our spin-torque diodes to the 50 Ω transmission line through which microwave power is applied, and hence, the maximum expected sensitivity can be further improved by adding a simple on-chip impedance matching transformer.

In conclusion, we fabricated the spin-torque diodes by optimizing the interfacial perpendicular magnetic anisotropy field between the MgO tunnel barrier and the $\text{Co}_{20}\text{Fe}_{60}\text{B}_{20}$ free layer. By applying the d.c. bias current, the detection voltages were significantly enhanced. At optimal conditions, we demonstrate a huge sensitivity of 210 kV/W in the absence of the magnetic field. Our results suggest that the injection locking mechanism combined with a proper design of MTJs can definitively be the basis for a commercial route of spintronics in microwave signal detection.

See [supplementary material](#) for the additional data from the devices with different CoFeB free layer thicknesses.

This work was supported by the Executive Programme of Scientific and Technological Cooperation Between Italy and China for the years 2016–2018 (code CN16GR09, 2016YFE0104100) titled “Nanoscale broadband spin-transfer-torque microwave detector” funded by the Ministero degli Affari Esteri e della Cooperazione Internazionale. This work was supported in part by the National Science Foundation of China (Nos. 51761145025 and 11474311) and the National Postdoctoral Program for Innovative Talents (No. BX201700275). The authors thank Steven Louis from Oakland University for his help and useful discussions.

¹J. C. Slonczewski, *J. Magn. Magn. Mater.* **159**, L1 (1996).

²L. Berger, *Phys. Rev. B* **54**, 9353 (1996).

³S. I. Kiselev, J. C. Sankey, I. N. Krivorotov, N. C. Emley, R. J. Schoelkopf, R. A. Buhrman, and D. C. Ralph, *Nature* **425**, 380 (2003).

⁴Z. Zeng, G. Finocchio, and H. Jiang, *Nanoscale* **5**, 2219 (2013).

⁵A. A. Tulapurkar, Y. Suzuki, A. Fukushima, H. Kubota, H. Maehara, K. Tsunekawa, D. D. Djayaprawira, N. Watanabe, and S. Yuasa, *Nature* **438**, 339 (2005).

⁶J. C. Sankey, Y.-T. Cui, J. Z. Sun, J. C. Slonczewski, R. A. Buhrman, and D. C. Ralph, *Nat. Phys.* **4**, 67 (2008).

⁷H. Kubota, A. Fukushima, K. Yakushiji, T. Nagahama, S. Yuasa, K. Ando, H. Maehara, Y. Nagamine, K. Tsunekawa, D. D. Djayaprawira, N. Watanabe, and Y. Suzuki, *Nat. Phys.* **4**, 37 (2008).

⁸J. Zhu, J. Katine, G. Rowlands, Y.-J. Chen, Z. Duan, J. Alzate, P. Upadhyaya, J. Langer, P. Amiri, K. L. Wang, and I. Krivorotov, *Phys. Rev. Lett.* **108**, 197203 (2012).

⁹T. Nozaki, Y. Shiota, S. Miwa, S. Murakami, F. Bonell, S. Ishibashi, H. Kubota, K. Yakushiji, T. Saruya, A. Fukushima, S. Yuasa, T. Shinjo, and Y. Suzuki, *Nat. Phys.* **8**, 491 (2012).

¹⁰S. Tsunegi, K. Yakushiji, A. Fukushima, S. Yuasa, and H. Kubota, *Appl. Phys. Lett.* **109**, 252402 (2016).

¹¹A. V. Nazarov, H. M. Olson, H. Cho, K. Nikolaev, Z. Gao, S. Stokes, and B. B. Pant, *Appl. Phys. Lett.* **88**, 162504 (2006).

- ¹²K. V. Thadani, G. Finocchio, Z. P. Li, O. Ozatay, J. C. Sankey, I. N. Krivorotov, Y. T. Cui, R. A. Buhrman, and D. C. Ralph, *Phys. Rev. B* **78**, 024409 (2008).
- ¹³A. M. Deac, A. Fukushima, H. Kubota, H. Maehara, Y. Suzuki, S. Yuasa, Y. Nagamine, K. Tsunekawa, D. D. Djayaprawira, and N. Watanabe, *Nat. Phys.* **4**, 803 (2008).
- ¹⁴Z. M. Zeng, P. Upadhyaya, P. Khalili Amiri, K. H. Cheung, J. A. Katine, J. Langer, K. L. Wang, and H. W. Jiang, *Appl. Phys. Lett.* **99**, 032503 (2011).
- ¹⁵W. H. Rippard, A. M. Deac, M. R. Pufall, J. M. Shaw, M. W. Keller, S. E. Russek, G. E. W. Bauer, and C. Serpico, *Phys. Rev. B* **81**, 014426 (2010).
- ¹⁶Z. M. Zeng, P. K. Amiri, I. N. Krivorotov, H. Zhao, G. Finocchio, J.-P. Wang, J. A. Katine, Y. M. Huai, J. Langer, K. Galatsis, K. L. Wang, and H. W. Jiang, *ACS Nano* **6**, 6115 (2012).
- ¹⁷H. Kubota, K. Yakushiji, A. Fukushima, S. Tamaru, M. Konoto, T. Nozaki, S. Ishibashi, T. Saruya, S. Yuasa, T. Taniguchi, H. Arai, and H. Imamura, *Appl. Phys. Express* **6**, 103003 (2013).
- ¹⁸H. Maehara, H. Kubota, Y. Suzuki, T. Seki, K. Nishimura, Y. Nagamine, K. Tsunekawa, A. Fukushima, A. M. Deac, K. Ando, and S. Yuasa, *Appl. Phys. Express* **6**, 113005 (2013).
- ¹⁹S. Miwa, S. Ishibashi, H. Tomita, T. Nozaki, E. Tamura, K. Ando, N. Mizuochi, T. Saruya, H. Kubota, K. Yakushiji, T. Taniguchi, H. Imamura, A. Fukushima, S. Yuasa, and Y. Suzuki, *Nat. Mater.* **13**, 50 (2014).
- ²⁰S. Tsunegi, T. Taniguchi, K. Yakushiji, A. Fukushima, S. Yuasa, and H. Kubota, *Appl. Phys. Express* **11**, 053001 (2018).
- ²¹B. Fang, M. Carpentieri, X. J. Hao, H. W. Jiang, J. A. Katine, I. N. Krivorotov, B. Ocker, J. Langer, K. L. Wang, B. S. Zhang, B. Azzerboni, P. K. Amiri, G. Finocchio, and Z. M. Zeng, *Nat. Commun.* **7**, 11259 (2016).
- ²²A. A. Timopheev, R. Sousa, M. Chshiev, H. T. Nguyen, and B. Dieny, *Sci. Rep.* **6**, 26877 (2016).
- ²³W. H. Rippard, M. R. Pufall, S. Kaka, T. J. Silva, S. E. Russek, and J. A. Katine, *Phys. Rev. Lett.* **95**, 067203 (2005).
- ²⁴X. Cheng, J. A. Katine, G. Rowlands, and I. N. Krivorotov, *Appl. Phys. Lett.* **103**, 082402 (2013).